Introduction to: Broadband FMR Spectroscopy

Application Note

Magnetic thin films not only form the backbone of fundamental spintronics and magnonics research, but are also constituents of current and future technologies focused on magnetic memory, sensors, logic, and microwave signal processing. Complimentary to conventional quasi-static techniques commonly employed for magnetic thin film characterization, e.g. magnetization hysteresis loop analysis via vibrating sample magnetometry, probing the microwave magnetization *dynamics* of thin films allows for additional material parameters to be measured, including the gyromagnetic ratio (γ), damping (α), inhomogeneous broadening (ΔHo), exchange stiffness (A), etc. which are not accessible by static measurement techniques.

Ferromagnetic resonance (FMR) spectroscopy has been carried out using microwave cavities since the late 1950's, typically on bulk samples. However, such microwave cavities are often tuned to a single resonance frequency. Over the last decade, the advent of *broadband* [1] FMR spectroscopy, using either stripline or coplanar waveguides, has allowed for measurements continuously spanning several 10's of GHz. Such broadband measurements allow for significant improvements in accurately extracting the aforementioned material parameters. More specifically, broadband measurements are necessary for analyzing the frequency dependence of the resonance linewidth and distinguishing between intrinsic and extrinsic contributions to the magnetic damping.

This application note will briefly describe the fundamental physics behind microwave magnetization dynamics, describe how broadband FMR measurements are performed and analyzed, and finally conclude with several measurement examples using the FMR spectrometer from NanOsc Instruments AB.

Magnetization dynamics: Landau-Lifshitz-Gilbert Equation

The classical description of microwave magnetization dynamics is provided by the Landau-Lifshitz-Gilbert (LLG) equation [2], shown in Figure 1, where $\hat{\mathbf{m}}$ is the magnetization vector, γ is the gyromagnetic ratio, μ_0 is the permeability of free space, H_{eff} is the effective magnetic field, and α is the phenomenological Gilbert damping coefficient. The term in blue describes the steady-state precession of the magnetization vector around H_{eff}. In the absence of any viscous forces, the magnetization vector would precess indefinitely along the dashed blue trajectory indicated in Figure 1. However, dissipative forces, shown in red and quantified by the phenomenological Gilbert damping coefficient α, will cause the magnetization to spiral inwards along the red dotted trajectory and eventually point collinear with H_{eff}. An FMR spectrometer provides the means to both stimulate and measure such magnetization dynamics.

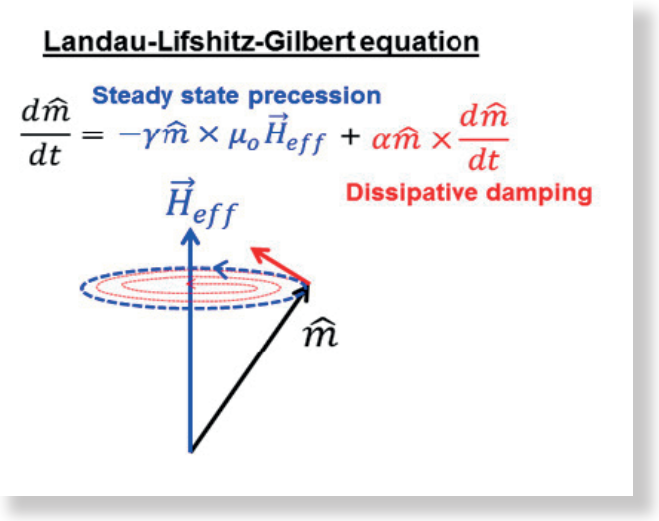

Figure 1: Magnetization dynamics as described by the Landau-Lifshitz-Gilbert equation.

Quantum Design

Quantum Design
1 avenue de l'Atlantique
Bâtiment Fuji-Yama
91940 Les Ulis - France

Tél. : +33 1 69 19 49 49
france@qd-europe.com
www.qd-europe.com

NanOsc Instruments

Experimental setup

The heart of a broadband FMR spectroscopy measurement setup, shown in Figure 2(a), is the coplanar waveguide (CPW). The role of the CPW is to efficiently transmit a microwave signal from a radio frequency (RF) source over a broad range of frequencies. CPWs provided by NanOsc Instruments AB can transmit frequencies ranging from 2-40 GHz. In close vicinity to the CPW a microwave RF magnetic field (H_{RF}) is generated which, at an appropriate magnetic field (H_{DC}) and frequency, can resonantly excite a magnetic sample. As the RF magnetic fields do not extend far from the CPW, it is important that the magnetic films be placed film side down on the CPW to maximize coupling and the resulting signal. It is also important that the sample does not short-out the CPW to itself. Therefore, a thin insulating layer (e.g. sputtered SiOx or spin-coated photoresist) is often deposited on the sample. One can also place a single layer of transparent tape on the CPW to provide an insulating barrier. The most efficient excitation mechanism is provided if H_{RF} is perpendicular to the magnetization of the sample, and therefore H_{RF} should be perpendicular to H_{DC}, as shown in Figure 2(a). Measurements are typically performed at a fixed frequency while sweeping H_{DC} to eliminate the dominant frequency dependent background response that may mask the relatively weak FMR response of the sample. As H_{DC} is swept through the resonance condition, the magnetization will begin to resonantly precess and will therefore absorb energy from the CPW. This decrease in transmitted RF energy when sweeping through the resonance field is converted to a DC voltage by a broadband RF diode. Such a schematic S21 absorption response is shown with the red curve in Figure 2(b). In order to improve the signal-to-noise ratio (SNR), a lock-in detection technique is often employed, which requires modulating the signal at a known frequency. This modulation is provided by an additional set of Helmholtz coils powered by an AC source which in-turn produces a small (~1 Oe) modulation (H_{AC}) to the much larger H_{DC}. Therefore, with this modified measurement scheme one actually measures the derivative of the transmitted power (dP/dH_{DC}), schematically shown in Figure 2(b) in blue. The electronic components (AC Source, RF Source, RF Diode, and Lock-in) shown in Figure 2(a) are conveniently housed and integrated together within the NanOsc FMR spectrometer, Figure 2(c), along with the electronics necessary to control and read (via a calibrated Hall sensor) the magnetic field (not shown).

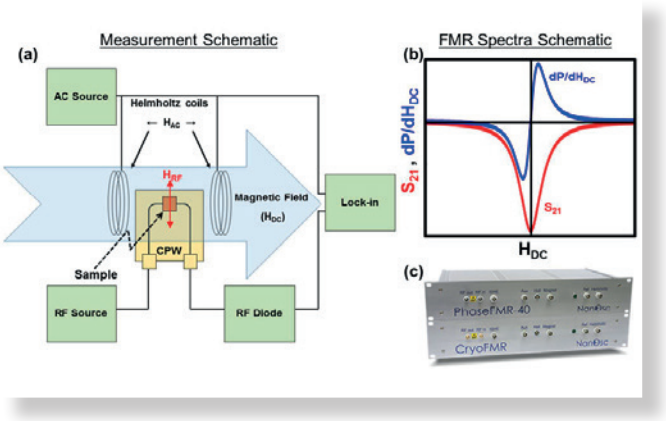

Figure 2: (a) Schematic broadband FMR measurement setup highlighting the critical components. (b) Schematic measurement spectra. (c) NanOsc FMR spectrometers.

Fitting the resonance spectra: Extracting resonance field and linewidth

A typical experimental resonance spectrum measured for a 2 nm thick $Co_{40}Fe_{40}B_{20}$ film at a resonance frequency of 6 GHz is shown in Figure 3(a, black squares) as a function of the in-plane magnetic field. The experimental data is then fit, Figure 3(a, red line) using the FMR spectrum fit equation, shown in Figure 2(a), in order to extract the resonance field (H_{res}) and linewidth (ΔH) at a particular frequency. This equation takes into account loading of the CPW when sweeping through the resonance condition and is therefore not a simple derivative of a Lorentzian function [3]. It also takes into account small linear backgrounds and vertical offsets. The extracted H_{res} and ΔH for frequencies up to 40 GHz are shown in Figure 3(b) and (c), respectively, along with the associated equation used to fit the data in order to extract $\mu_o M_S$, ΔH_o, and α.

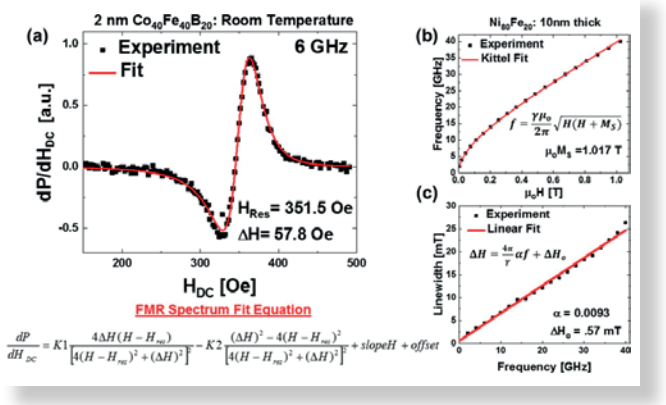

Figure 3: (a) Experimental resonance spectrum (black squares) with fit (red line) to extract the resonance field and linewidth at f=6 GHz for a 2 nm thick $Co_{40}Fe_{40}B_{20}$ film. The extracted (b) resonance field and (c) linewidth shown as black squares over the frequency range of 2→40 GHz, along with the associated fits (red lines) used to calculate $\mu_o M_S$, ΔH_o, and α.

Quantum Design

Quantum Design
1 avenue de l'Atlantique
Bâtiment Fuji-Yama
91940 Les Ulis - France

Tél. : +33 1 69 19 49 49
france@qd-europe.com
www.qd-europe.com

NanOsc Instruments

Measurement Examples:

(i) Film quality after post annealing:

The extracted frequency dependence of the resonance field and linewidth of a Pd(8)/Cu(15)/Co(8)/Cu(8)/$Ni_{80}Fe_{20}$(4.5)/Cu(3)/Pd(3)(thicknesses in nm) pseudo spin valve multilayer film stack are shown in Figure 4. While the film stack contains two ferromagnetic layers, namely Co and $Ni_{80}Fe_{20}$, only the resonance field and linewidth of the $Ni_{80}Fe_{20}$ layer is shown. Three measurements are taken. The first is of the as-deposited virgin film stack, which shows the highest saturation magnetization and lowest damping. However, after two subsequent post-annealing processes of the film stack (200 °C for 12 hours) the FMR measurements reveal a subtle decrease in saturation magnetization and a dramatic increase in damping. These changes are attributed to structural changes within the $Ni_{80}Fe_{20}$ film upon heat treatment and interdiffusion of the nearby Cu layers into the $Ni_{80}Fe_{20}$ [4].

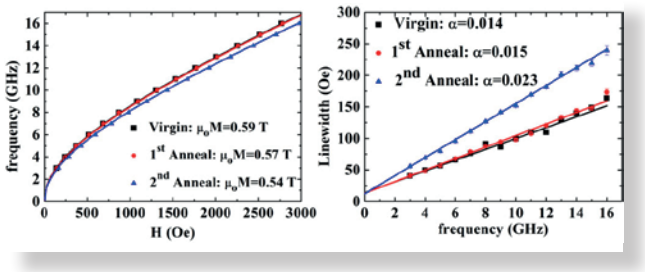

Figure 4: The extracted frequency dependence of the resonance field and linewidth of a pseudo spin valve multilayer film stack. The as-deposited virgin data (black symbols and lines) shows clear changes from subsequent annealed films (red and blue symbols and lines). Figure reprinted with permission [4].

(ii) Extracting MS, α, and A of alloy films:

In addition to the uniform FMR precession described before where all the of the spins precess in phase through the film thickness, additional higher order spin wave modes can be excited in thin film samples. For example, a perpendicular standing spin wave (PSSW) mode, schematically shown in Figure 5(a), can be excited and can be readily measured in relatively thick films (> 50 nm) using broadband FMR spectroscopy. As shown in Figure 5(b), two resonances can be observed and correspond to the FMR and PSSW modes. Note, for a fixed frequency, the PSSW mode will occur at a lower field than the FMR mode. As described in Yin et al, by fitting the resonance field of the PSSW mode the exchange stiffness constant, *A*, can also be measured. The model system presented in Figure 5 is 100 nm thick Permalloy (Py) films alloyed with a noble metal, more specifically $Py_{100-x}M_x$, where M = Pt, Au, or Ag. The damping, α, saturation magnetization, M_S, and exchange stiffness, *A*, are shown in Fig. 5(c) as a function of noble metal concentration. Generally, the addition of Pt, Au, and Ag into Py tends to increase damping and decrease the saturation magnetization and exchange stiffness. Most interestingly, it was found that the addition of Ag, which dramatically decreased both M_S and *A*, had only a small effect on α [5].

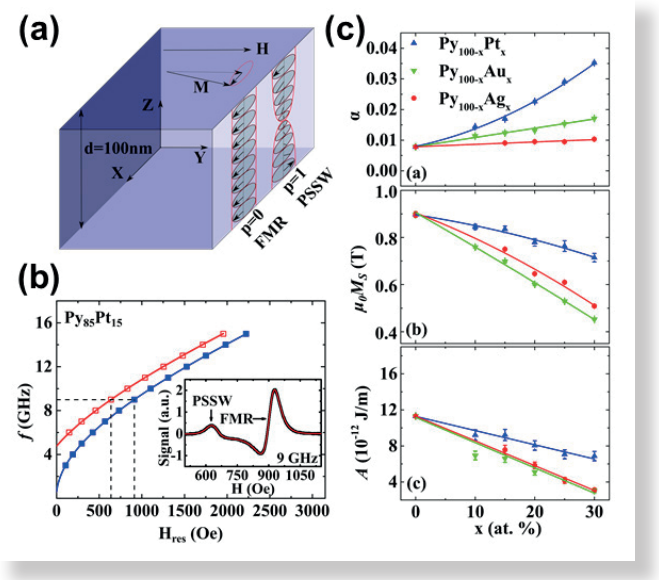

Figure 5: (a) Schematic representation of the FMR and PSSW modes in a magnetic film. (b, inset) A single experimental field-swept spectra and fit for f=9 GHz, which clearly shows both the FMR and PSSW resonances. (b, main panel) Extracted frequency dependence of the resonance field of the FMR (in blue) and PSSW (in red) modes for a 100 nm thick Py85Pt15 film. (c) Compositional dependence of the damping, α, saturation magnetization, MS, and exchange stiffness, A. Figure reproduced with permission [5].

(iii) Temperature dependence studies:

The ability to measure FMR spectra at various temperatures is also critically important to the physics and materials science communities as the temperature dependence of the saturation magnetization, damping, and inhomogeneous broadening provide further insight into the fundamental dynamics. The CryoFMR probe for use in a Quantum Design Physical Properties Measurement System (PPMS) or DynaCool allows for easy and automated measurements over the temperature range of 4→400 K. Note: A similar probe for the VersaLab measurement platform allows for measurements ranging from 55→400 K.

Figure 6(a) shows a family of measurement spectra showing both the FMR and PSSW modes for a 100 nm thick $Py_{85}Au_{15}$ film spanning a wide temperature range. The inset of Figure 6(a) shows the extracted linewidth of the FMR mode, used to calculate the magnetic damping, for two different temperatures. Figure 6(b) then shows the extracted temperature dependence of the spin wave stiffness D (a parameter related to the exchange stiffness A) for a variety of different alloys. Finally, Figure 6(c) shows the temperature dependence of the saturation magnetization, damping, and inhomogeneous broadening for three ferromagnetic thin film samples with only minor differences in composition and deposition conditions. Interestingly, for only subtle differences in the three samples, dramatic differences, in both magnitude and trends, in the temperature dependence are observed.

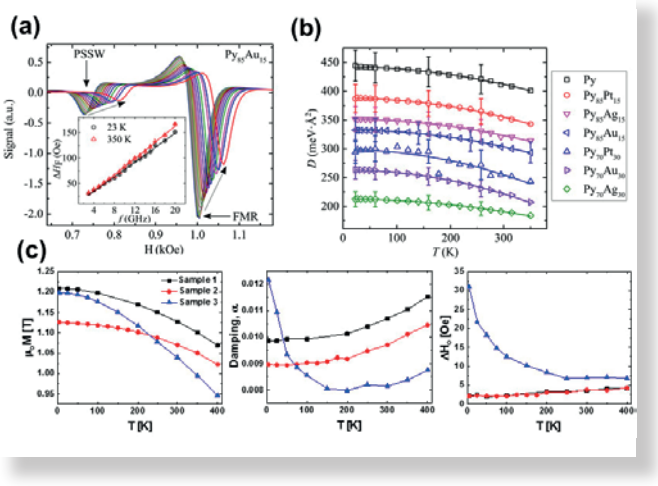

Figure 6: (a, main panel) Family of resonance spectra for temperatures spanning 23-350 K. (a, inset) Frequency dependence of the linewidth of the FMR mode for two different temperatures. (b) Temperature dependence of the spin wave stiffness for a variety of Py based alloys. Figure reprinted with permission [6]. (c) Temperature dependence of M_s, α, and ΔH_o for three ferromagnetic thin film samples provided courtesy of Dr. Susumu Okamura from Western Digital.

(iv) Inverse spin Hall effect (ISHE):

If we consider a ferromagnet/non-magnetic bilayer (e.g. $Ni_{80}Fe_{20}$/Pd) undergoing FMR, a diffusive flow of spin from the $Ni_{80}Fe_{20}$ ferromagnet will enter the non-magnetic Pd layer due to a phenomenon known as spin pumping [7].Then, via the inverse spin Hall effect (ISHE) [8], which can be significant in non-magnetic layers with a large spin-orbit interaction (e.g. Pt, W, Pd, etc.), this diffusive flow of spins will be converted into a measurable transverse DC voltage. A special CPW, shown in Figure 7(a), integrates electrical contacts for measuring this ISHE generated voltage (V_{ISHE}) and are connected to a separate input on the NanOsc FMR spectrometer. The ISHE voltage is measured using the same lock-in amplifier used to measure the FMR response. However, for ISHE measurements two different modulation schemes are provided. One can either (i) modulate the external field using the provided Helmholtz coils, as is done when measuring the FMR response, or (ii) chop/pulse the V_{ISHE} using an internal relay. Both modulation schemes are shown in Figure 7(b) for a $Ni_{80}Fe_{20}$/Pd bilayer. Note that the field-modulated response has a similar derivative-like curve shape, while the pulse-modulated signal exhibits a single peak and improved SNR as compared to the field-modulated signal.

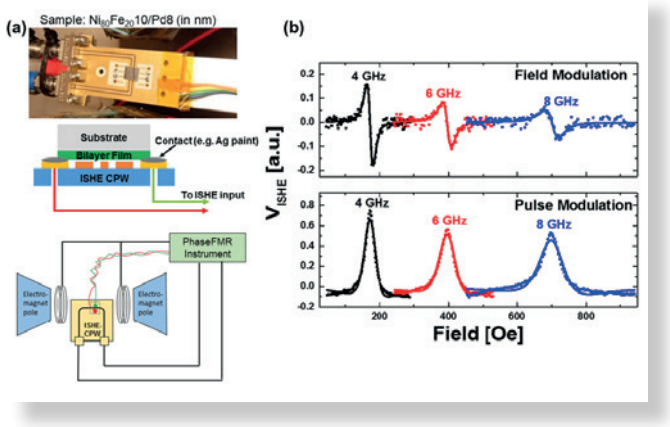

Figure 7: (a) Experimental design of ISHE measurements utilizing a special CPW which incorporates electrical contacts. (b) Measured VISHE responses of a $Ni_{80}Fe_{20}$/Pd bilayer for three representative frequencies employing either the field-modulated (top) or pulse-modulated (bottom) detection scheme.

Quantum Design

Quantum Design
1 avenue de l'Atlantique
Bâtiment Fuji-Yama
91940 Les Ulis - France

Tél. : +33 1 69 19 49 49
france@qd-europe.com
www.qd-europe.com

NanOsc Instruments

Conclusion

In summary, broadband FMR spectroscopy measurements of thin films allows for a variety of material parameters to be measured that are not feasible by more conventional static techniques. The above examples give a brief introduction to many diverse material systems highlighting the utility of broadband FMR. For more measurement examples, specifically using the NanOsc line of FMR spectrometers, please see [10] for the most current updates.

References

[1] I. Maksymov and M. Kostylev, "Broadband stripline ferromagnetic resonance spectroscopy of ferromagnetic films, multilayers and nanostructures", Physica E 69, 253 (2015).
[2] A. Gurevich and G. Melkov, "Magnetization oscillations and waves", CRC Press, Boca Raton, 1996.
[3] G. Woltersdorf, Ph.D. thesis, Simon Fraser University, 2004.
[4] A. Houshang, et al., "Effect of excitation fatigue on the synchronization of multiple nanocontact spin-torque oscillators", IEEE Magnetics Letters 5, 3000404 (2014).
[5] Y. Yin, et al., "Tunable permalloy-based films for magnonics devices", Physical Review B 92, 024427 (2015).
[6] Y. Yin, et al., "Ferromagnetic and spin-wave resonance on heavy metal doped permalloy films: temperature effects", IEEE Magnetics Letters 8, 3502604 (2017).
[7] Y. Tserkovnyak, A. Brataas, G.E.W Bauer, "Enhanced Gilbert damping in thin ferromagnetic films", Physical Review Letters 88, 117601 (2002).
[8] J.E. Hirsch, "Spin Hall Effect", Physical Review Letters 83, 1834 (1999).
[9] E. Saitoh et al., "Conversion of spin current into a charge current at room temperature: inverse spin-Hall effect" Applied Physics Letters 88, 182509 (2006).
[10] For additional measurement examples see: http://www.nanosc.se/testimonials.html